arXiv:0809.2484v1 [astro-ph] 15 Sep 2008

TWO DISTINCT PHASES OF HARD X-RAY EMISSIONS IN A SOLAR ERUPTIVE FLARE

Bhuwan Joshi[1], Astrid Veronig[2], K. -S. Cho[1], S. -C. Bong[1], Y. -J. Moon[3], Jeongwoo Lee[4], B. V. Somov[5], P. K. Manoharan[6], Y. -H. Kim[1]

joshi@kasi.re.kr

ABSTRACT

We present a detailed analysis of the evolution of an M7.6 flare that occurred near the south-east limb on October 24, 2003 utilizing a multi-wavelength data set. Preflare images at TRACE 195 Å show that the bright and complex system of coronal loops already existed at the flaring site. The X-ray light curves clearly reveal two phases of flare evolution. The emission during the first phase is seen in GOES and RHESSI measurements at energies below 25 keV, while the second phase is evident in all the X-ray energies as high as 300 keV. The first phase is gradual whereas the second phase shows impulsive emission with several individual hard X-ray bursts. The first phase starts with the appearance of an X-ray loop-top (LT) source in RHESSI images below 25 keV. About 5 minute later, the TRACE 195 Å images show an intense emission that is cospatial with RHESSI LT source. This hot and diffuse TRACE emission is attributed to the existence of 15-20 MK plasma, heated directly from the primary energy source. Both X-ray and TRACE LT sources exhibit an altitude decrease for ~ 11 minute. The high energy X-ray emission between 25-300 keV dominates the second phase, which correlates well with TRACE 1600 Å and Hα flare ribbons. The first phase seems to be mostly dominated by hot thermal emission from flaring loops with temperatures $T > 25$ MK. The second phase is found to be dominantly non-thermal in

[1]Korea Astronomy and Space Science Institute, Daejeon 305-348, Korea

[2]IGAM/Institute of Physics, University of Graz, Universität splatz 5, A-8010 Graz, Austria

[3]Department of Astronomy and Space Science, Kyung Hee University, Yongin 446-701, Korea

[4]Physics Department, New Jersey Institute of Technology, 161 Warren Street, Newark, NJ 07102

[5]Astronomical Institute, Moscow State University, Universitetskij Prospekt 13, Moscow 119992

[6]Radio Astronomy Centre, Tata Institute of Fundamental Research, Udhagamandalam (Ooty) 643 001, India

nature, with distinct emission from hard X-ray footpoints and the spectra at high energies follow hard power laws ($\gamma = 2.6 - 2.8$). The observations of the second phase are mostly consistent with the standard flare model while the results of the first phase contains evidence for the collapsing trap effect in solar flare.

Subject headings: Sun: corona — Sun: flares — Sun: X-rays

1. Introduction

The active Sun displays a stunning variety of transient energetic phenomena ranging from the smallest microjets and microflares to the largest flares and coronal mass ejections (CMEs). It is generally accepted that the energy released during flares and CMEs is stored in the corona prior to the event in the form of stressed or non-potential magnetic fields. We believe that this stored free energy in the coronal magnetic fields is released explosively through the process of magnetic reconnection. Multi-wavelength measurements of flares and CMEs made over the years have provided many valuable pieces of information about the response of coronal energy release in the different atmospheric layers of the Sun. During an eruptive flare, the whole magnetic configuration of coronal loops crossing an inversion line is disrupted and is followed by a newly rebuilt loop system from pre-flare to post-flare stages. The expansion of flare ribbons and growth of flare loop system are the clearest observational findings which support the flare models involving magnetic reconnection (for a review see Priest & Forbes 2002; Lin et al. 2003).

Yohkoh spacecraft significantly improved our overall understanding about the flare physics (Hudson et al. 2004). Observations made by Yohkoh confirmed the presence of hard X-ray sources at the footpoints of the loop system (Sakao 1994) and detected a new hard X-ray source above the apex of the hot flaring loop observed in soft X-rays (Masuda et al. 1994; see also Somov et al. 2005). The above-the-looptop source is believed to be intimately connected to the primary energy release site and location of the electron acceleration in the corona, again supporting the reconnection models. RHESSI spacecraft with superior observing capabilities in X-ray energy levels, further refined our knowledge about the X-ray looptop coronal source. It detected a downward motion of looptop source during the initial phase of impulsive rise of hard X-ray flux (Sui & Holman 2003; Sui et al. 2004; Liu et al. 2004; Ji at al. 2006; Veronig et al. 2006; Joshi et al. 2007). We still do not have a plausible explanation of this phenomenon. RHESSI observations have also revealed the existence of double coronal source, which is believed to be an indirect evidence for the formation and expansion of a large scale current sheet in the corona (Sui & Holman 2003; Sui et al. 2004; Sui et al. 2005; Liu et al. 2008).

In this paper we present a comprehensive multi-wavelength analysis of an M 7.6 flare on 2003 October 24. A detailed X-ray imaging and spectroscopic analysis of RHESSI observations clearly exhibit two distinct phases of flare evolution in view of the X-ray energy release process. The first stage is gradual and dominated by thermal emission while the second stage is impulsive with mainly non-thermal characteristics. A significant and unusually long downward motion of the loop-top source characterizes the first phase. During the whole second phase we find the evolution of the so-called standard foot-point sources and upward expansion of loop-top source. The event was associated with a fast CME. We compare flare observations at different X-ray wavelengths, and also with other chromospheric and coronal images with the aim to study the consequences of the magnetic reconnection process at various atmospheric layers. In section 2, we describe the observational characteristics of the event. We interpret our observational findings in the final section of the paper.

2. Observations and Results

Figure 1 shows the soft X-ray (SXR) flux recorded by the GOES satellite in the 0.5–4 and 1–8 Å wavelength bands between 02:00 to 03:40 UT. GOES measurements reveal this flare to be a typical long duration event lasting from 02:15 to about 05:00 UT with a maximum around 02:53 UT. The Reuven Ramaty High Energy Solar Spectroscopic Imager (RHESSI; Lin et al. 2002) made a complete coverage of this long duration event. The Transition Region and Coronal Explorer (TRACE; Handy et al. 1999) had obtained image sequences in 195 Å and 1600 Å wavelengths of the activity site during various phase of the flare evolution. In the following subsections we analyze these observations in detail.

2.1. X-ray time profiles: two phase evolution

The GOES flux starts to increase steadily from 02:16 UT and attained the first peak at 02:40 UT (Fig. 1). The flux then shows a decreasing trend and then further increases after 02:45 UT. The overall maximum is achieved in both the GOES channels at 02:53 UT. In Figure 2 various X-ray light curves of the flare are presented. The top panel shows the GOES SXR flux while the other panels present the time histories in five different X-ray energy bands utilizing RHESSI spacecraft observations. The comparison of different time profiles clearly reveal two phases of the flare evolution: a first phase between 02:24 and 02:44 UT, which is clearly manifested in GOES and RHESSI 6–25 keV light curves followed by a second phase. The second phase of emission is seen in all the energy bands in GOES as well as RHESSI. The first phase is gradual while the second phase shows impulsiveness with

several hard X-ray bursts. Here it is important to notice that the first phase of emission is completely absent in high energy bands above 50 keV. The second phase of emission peaked at 02:48 UT in all the hard X-ray bands from 12 to 300 keV. The hard X-ray emission at the second phase is characterized by four prominent bursts at 02:45, 02:48, 02:51, and 02:56 UT (marked by A, B, C, and D respectively in Fig. 2e) which appear roughly simultaneously at all energies from 25 to 300 keV. These hard X-ray bursts appear to be more prominent as the light curves at higher energies are considered.

Here it is relevant to mention that the LASCO onboard SOHO (Brueckner et al. 1995) detected a fast CME associated with this flare event. The height-time plot available at SOHO–LASCO–CME catalogue[1] shows the mean propagation speed of CME in LASCO field of view is about 1055 km s^{-1}. The CME first appeared in LASCO C2 coronagraph at 02:54 UT at a radial distance of $\sim$2.7 $R_\odot$. The extrapolation of CME height backward in time suggests its association with the first phase of the flare evolution.

2.2. X-ray, (E)UV and Hα imaging

The RHESSI images have been reconstructed with the CLEAN algorithm with the natural weighing scheme using front detector segments 3 to 8 in different energy bands, namely, 6–12, 10–15, 25–50, 50–100, and 100-300 keV (Hurford et al. 2002). We compare RHESSI measurements with TRACE images in 195 and 1600 Å wavelengths. The TRACE 1600 Å channel is sensitive to plasma in the temperature range between (4–10)$\times10^3$ K. Emissions at this wavelength originate mainly from the chromosphere and provide valuable informations about the chromospheric response to the coronal energy release. The TRACE 195 Å channel is sensitive to higher temperature [(5.0–20)$\times10^5$ and (1.1–2.6)$\times10^7$ K] plasma and show relatively low temperature coronal structures which develop during the flare evolution (Handy 1999).

First, we discuss the flare characteristics during the first phase of evolution (i.e., between 02:24 and 02:45 UT) prominent in GOES profile and RHESSI measurements at low energies ($\lesssim$ 25 keV). The sequence of RHESSI images in 6–12 and 12–25 keV energy bands show a bright looptop (LT) source which develops right at the flare onset. The LT source then shows shift to lower altitudes. Images in both the energy bands reveal similar morphological and temporal evolution of looptop source. In Fig. 3, four representative 6–12 keV images during this period are shown. At the flare onset, a looptop source and associated coronal loop are seen. The looptop source appeared above the limb while the loop system extends to

[1]http://cdaw.gsfc.nasa.gov/CME_list/

the disk with northern leg apparently longer than the southern one (top left panel of Fig. 3). In the later stages, the loop system shrinks and the looptop structure continues to become more compact and brighter.

A bright and complex system of parallel loops already pre-existed and was observable in TRACE 195 Å images at the activity site before the flare onset (first panel of Fig. 4). RHESSI looptop source, which appeared as early as ∼02:24 UT, is located at the top of the northern side of TRACE loop system (Fig. 5). Intense brightening occurred at the top of TRACE loops from 02:29 UT onwards and the loops start to shrink (Figs. 4 and 5). In Fig. 6 we present the altitude evolution of the LT source derived from RHESSI 6–25 keV measurements and TRACE 195 Å images. Here, the LT altitude is defined as the distance, along the main axis of motion, between the centroid of the LT and the center of the line between the two FP seen in RHESSI 50–100 keV energy band in later stages. We find that the TRACE and RHESSI looptop sources are almost co-spatial in the course of downward motion from 02:29 to 02:35 UT (see also Fig. 5). During this interval, the RHESSI 6–12 and 12–25 keV LT sources reveal a mean downward velocity of 15 and 14 km s^{-1} respectively while for TRACE LT source the mean downward velocity is 16 km s^{-1}. We further note that the downward motion of the RHESSI LT source is observed during the gradual rise of X-ray fluxes at low energies (< 25 keV). Here it is interesting to notice that the X-ray emission at high energies (> 50 keV) starts in the later stages ($>$ 02:44 UT), several minutes after the end of downward motion of X-ray LT source.

The second phase of flare evolution (i.e., between 02:45 to 03:14 UT) is marked by four peaks in hard X-ray light curves in different energy bands from 25 to 300 keV (Fig. 2). Figure 7 shows the RHESSI images in 10–15, 25–50, 50–100, and 100–300 keV energy bands at the time of four peaks (denoted by A, B, C, and D in Figs. 2 and 7). The hard X-ray images in all the three energy bands above 25 keV first show a bright hard X-ray source around the first peak (A). Another source developed southward of the first one during the second peak (B), which coincide with the overall flare maximum in high energy channels ($>$ 12 keV). These two sources lie over the two bright flare ribbons observed at 1600 Å TRACE images (Fig. 8). Therefore, we interpret these two sources as the northern and southern footpoints of a loop system, the looptop of which is clearly visible in RHESSI images at energies below 25 keV (Figs. 7 and 8). We note that most of the time the northern footpoint (FP) remains brighter than southern one. However, the intensity of southern FP increases slowly with time and near the end of the second phase both the FPs are of similar brightness.

We note that the evolution of the LT source after 02:35 UT is rather complicated. Examination of both 6–12 and 12–25 keV images shows that the height of LT source does not change for the next few minutes before showing the commonly observed upward expansion

(Fig 6). The X-ray LT source at 12-25 keV start moving upward ∼3 minutes earlier than the 6-12 keV LT source. Here we should bear in mind that 12-25 keV source observes hotter plasma than 6-12 keV source. We also notice that during the upward expansion, the LT source at 12–25 keV is located at higher altitudes than LT source in 6–12 keV (i.e. the emission at higher temperature comes from higher altitude). For upward motion, we obtained mean velocities of 23 and 17 km s^{-1} for 6–12 (between 02:49–03:00 UT) and 12–25 keV (between 02:46–03:00) sources respectively. Another interesting feature during the upward motion of X-ray LT source is the increase in the brightness at the top of a nearby loop system (seen in TRACE 195 Å images; see image at 02:58:59 UT in Fig. 5) situated at the southern side of the main LT source. The evolution history of the new southern LT source can be nicely seen in Figure 9. In the later stages, the brightness of southern LT source increases and start dominating over the northern main looptop source (Fig. 9). The TRACE 195 Å LT source with bright, diffuse emission exhibits little downward motion between 02:35 and 02:50 UT (Figs. 4 and 6) with a mean velocity of 3 km s^{-1}. In the later stages (> 02:54 UT), the bright emission seen in TRACE 195 Å images is more structured and spread along the loop, below which dark (and cool) system of post-flare loops is visible (Figure 4). The loop system shows an upward expansion with a mean velocity of 5 km s^{-1}.

In the bottom panel of Figure 6, we have shown the temporal evolution of plasma temperature derived from GOES 12 observations. We find that the plasma temperature is higher during the first phase and attains the maximum value at ∼02:34 UT. Further we find that the decrease of LT source altitude is anti-correlated with plasma temperature evolution during the first phase (between 02:24 and 02:35 UT). After 02:34 UT plasma temperature decreases rapidly till ∼02:44 UT. In the beginning of the second phase the temperature remains nearly constants for several minutes (between ∼02:47 and ∼02:53 UT) while it decreases very slowly in the later stages.

The flare associated bright plasma structures observed in TRACE 195 Å images during the first and second phases need further attention. We stress that throughout the first phase, the intense, diffuse LT source, seen in TRACE 195 Å images near the looptop, is co-spatial with X-ray looptop source observed in 6-25 keV energies and shows similar altitude evolution. This diffuse emission is believed to be originated from hot 15-20 MK plasma in response to the presence of Fe XXIV (192 Å) resonance line which lies within the TRACE 195 Å passband (Warren & Reeves 2001). Warren & Reeves (2001) and Gallagher et al. (2002) also noticed similar flare associated high-temperature plasma structures. On the other hand, the bright, slowly expanding loop system seen in TRACE 195 Å images during the later stages (> 02:54 UT) lies below the upward moving RHESSI X-ray looptop source (Fig. 5). This suggests that now TRACE at 195 Å observes post-flare loop system and bright, structured emission along the loops indicates low temperature plasma structures (1.5

MK) dominating the TRACE 195 Å filter response. We also notice that between 02:50 and 02:54 UT the TRACE LT source shows fast downward motion with mean velocity of 19 km s^{-1}, which is quite different from the behaviour of RHESSI LT source (Fig. 6). This likely reflects the fact that during this interval in TRACE 195 Å images, we switch from 15-20 MK flare plasma to 1.5 MK post-flare loop system.

The TRACE images at 1600 Å and Hα filtergrams taken from ARIES Solar Tower Telescope, India (Pant 2006) during the decline phase (after 02:55 UT) reveal clear post-flare loop configuration that connects the flare ribbons (Figs. 8 and 10). We note that the Hα loops are seen in emission against the solar disk which is rather unusual and indicative of high densities in the post flare loops (in excess of 10^{12} cm^{-3}).

2.3. RHESSI X-ray spectroscopy

Figure 12 shows spatially integrated, background subtracted RHESSI spectra derived during nine time intervals of the flare (indicated in Fig. 11) together with the applied spectral fits. Each spectrum was accumulated over 80 s and derived with 1 keV energy bins from 10 to 200 keV using all RHESSI front detector segments except 2 and 7 (which have lower energy resolution and high threshold energies, respectively) and deconvolved with the full detector response matrix, i.e., including off-diagonal elements (see Smith et al. 2002). Due to the high count rates at low energies, the effect of pile-up is severe during this event, i.e. two (or more) low-energy photons arrive almost simultaneously at one detector and are recorded as a single photon with energy equal to the sum of the individual photon energies (Smith et al. 2002). We applied the pile-up correction implemented in the RHESSI software. However, we note that during the early phase (Fig. 12, panels a–c) where the spectra are very steep, this correction may not be fully satisfactory.

Spectral fits were obtained using a forward-fitting technique for which the functional form of the incident photon flux spectra is assumed for a parametric model of the source. Specifically, we used the bremsstrahlung spectrum of an isothermal plasma and a power-law function with a turn-over at low X-ray energies. The spectra shown in panels a–c of Fig. 12 were derived during the first phase of the flare. They are dominated by hot thermal emission with temperatures $T > 25$ MK already at the very start. At X-ray energies $\varepsilon \gtrsim 20$ keV, the spectrum shows a steep power-law, with photon spectral index $\gamma \gtrsim 7$. At this first phase of the flare, RHESSI images show emission mostly from the flaring loops, concentrated toward the loop tops. Only during one interval at 02:30–02:32 UT we briefly see HXR emission from footpoints (in 25–50 keV RHESSI images). At this time also the spectral index is harder with $\gamma = 5.7$ (see panel b in Fig. 12).

During the second phase of the flare, the spectra show quite different characteristics (see Fig. 12, panels d–i). Emission up to >200 keV from RHESSI footpoints is detectable above the background, and the spectrum at high energies follows hard power laws. Remarkably, the photon spectral index is almost the same for each of the individual peaks, with γ in the range 2.6–2.8. We also note that the thermal emission is not increasing any further in this second flare phase but temperature as well as emission measure reached their peaks already during the first phase (see Fig. 12).

3. Discussion

In the previous section, we present the evolution of a long duration M7.6 flare on 2003 October 24 in detail. TRACE images at 195 Å of flaring region show that the primary energy release took place in a complicated configuration of coronal loops.

The RHESSI count rates at low energies ($\leq$ 25 keV) and soft X-ray time histories by GOES clearly define two phases of flare evolution; first phase between 02:24 and 02:44 UT, followed by a second phase between 02:44 UT and 03:14 UT (Fig. 2). The first phase of emission is completely absent in X-ray time profiles above 50 keV. However, in 25–50 keV time profile a small flux enhancement can be seen during the first phase. All the time profiles between 25–300 keV clearly demonstrate four distinct hard X-ray bursts during the second phase (indicated by A, B, C, and D in Fig. 2e).

3.1. The first phase

The RHESSI images below 25 keV and TRACE 195 Å measurements reveal many unique observational findings during the first phase of flare evolution. The X-ray LT source appears right at the flare onset and starts moving to lower altitudes. The LT source is characterized by unusually long duration of LT altitude decrease (from 02:24 to 02:35 UT). About 5 minutes after the appearance of X-ray LT source, an intense brightening starts in TRACE 195 Å loops which is cospatial with RHESSI LT source. This diffuse TRACE LT source suggests that the initial energy release heated plasma directly to high temperature (15-20 MK) and is observed in Fe XXIV (192 Å) resonance line within TRACE 195 Å passband. We find that TRACE 195 Å LT source also shows a similar altitude decrease during this period (from 02:29 to 02:35 UT) and its speed of downward motion is comparable to that of RHESSI measurements. From RHESSI spectral analysis we conclude that during the first phase the emission from LT source is most probably thermal bremsstrahlung from plasma

with temperature T > 25 MK.

Li & Gan (2006) studied the LT evolution in M2.5 flare that occurred on 2002 April 16 using RHESSI and TRACE 195 Å observations. They found that in the early impulsive phase of ∼5 minutes, both TRACE and RHESSI LT sources showed decrease in altitude. The temporal behavior of TRACE source exhibited more consistency with RHESSI 12–25 keV source than 6–12 keV source. However, in our case the downward motion and corresponding speeds of the three sources (i.e. RHESSI 6–12, RHESSI 12–25 and TRACE 195 Å) are nearly similar. Further in the present event, the TRACE LT shrinkage is very obvious in direct images; Li & Gan (2006) detected loop shrinkage in running difference images. The downward motion of altitude decrease of LT source in the early phase of flare evolution has been established by many RHESSI observations (Krucker et al. 2003; Sui & Holman 2003; Sui et al. 2004; Liu et al. 2004; Ji et al. 2006; Veronig et al. 2006; Joshi et al. 2007; Liu et al. 2008). Some of the previously studied events also show energy dependent structure of LT source during the phase of altitude decrease, i.e. the higher energy sources were located higher in the corona and showed a faster speed of downward motion than lower energy sources (Sui et al. 2004; Veronig et al. 2006; Liu et al. 2008). In our event, however, the difference of LT altitude between the sources observed at low and high energy bands (i.e., 6–12 and 12–25 keV) is not significant during this stage. Further the LT altitude decrease is observed in RHESSI observations for ∼11 minutes, which is significantly larger than reported previously. Apart from RHESSI and TRACE observations, downward source motion is also observed in microwave flare images at 34 GHz (Li & Gan 2005). Many observational evidences supporting the altitude decrease of looptop source before the main phase of flare emission from X-ray, EUV and microwave measurements reveal this phenomenon to be a very crucial phase of flare evolution and associated closely with the magnetic reconnection process (cf. the discussion in Sui et al. 2004).

Finally we note that the duration of downward motion of the LT source is marked by high plasma temperature. RHESSI observations indicate that the plasma temperature ranges from 21−27 MK during this interval. We further notice that temperature reached to high values (∼27 MK) at the early stage. The temperature determined from GOES channels is lower (maximum temperature ≈ 20 MK) and shows gradual rise with the LT shrinkage. Large difference between temperature computed from RHESSI and GOES measurements could be due to different sensitivity and response of these two detectors. This is also consistent with the fact that the observed plasma is multi-temperature. These results suggest a possible connection between LT heating and loop contraction and could be interpreted in terms of "collapsing magnetic trap effect" (Somov & Kosugi 1997; Karlický & Kosugi 2004; Somov 2006; Veronig et al. 2006). In this scenario, hot plasma and frozen-in magnetic field flowing from the reconnection site creates the collapsing magnetic trap. The magnetic field

compression in this flow continue to heat the plasma to higher temperatures by the betatron mechanism and can form a region of super hot plasma at the loop-top (Karlický & Kosugi 2004). At least, the decrease in the volume of the trap during its contraction results in an increase in the density of the trapped particles and enhances the role of Coulomb collisions. Although the betatron effect does not change the total particle energy at the exit from the collapsing trap (Somov & Bogachev 2003), this energy is differently distributed between the thermal and non-thermal components in the source of hard X-ray radiation. Thus, in a future research of the flare on October 24, 2003, it is interesting to estimate a plasma density inside the collapsing magnetic trap.

3.2. The second phase

The flare evolution during the second phase (i.e., between 02:45 and 03:10 UT) shows impulsive hard X-ray emission at high energies. During this interval various observational signatures in Hα, (E)UV and hard X-ray wavelengths can be well explained by the standard CSHKP model of flare which is consistent with nearly all eruptive flare models. These observational features include: appearance of two parallel flare ribbons in TRACE 1600 Å and Hα images; two hard X-ray footpoints, one lying on each flare ribbons; growth of X-ray looptop source; formation of relatively cool loop system below X-ray looptop source at UV and Hα wavelengths connecting flare ribbons as well as post flare loop configuration observed in the later stages of gradual decline of X-ray intensity. There is no further increase in temperature during the second phase. The flat X-ray spectra observed during the second phase imply that this phase is mainly non-thermal, dominated by energy released into acceleration of electrons.

In all the high energy bands (25–300 keV), the light curves show four peaks (indicated by A, B, C, and D in Figs. 2 and 7). A comparison of their timings with flare images reveal a consistent picture. The first peak is characterized by a well developed bright footpoint which lies on the northern flare ribbon. The overall maximum of the time profile (i.e., the second peak in high energy X-ray profiles) is marked by the appearance of a second hard X-ray footpoint source which lies on the southern flare ribbon. However, the intensity of southern footpoint increases continuously after the flare maximum and eventually both the footpoints became of comparable brightness (Fig. 7). The consistency between the timings of peaks in light curves and morphological evolution of footpoint sources can be understood in terms of thick-target interpretation (Brown 1971; Hudson 1972; Syrovatskii & Shmeleva 1972) in which the X-ray production at the legs of the loop system takes place when high energy electrons, accelerated in the reconnection region, come along the guiding magnetic

field lines and slam the denser transition region and chromospheric layers producing hard X-ray emission via nonthermal bremsstrahlung produced by fast electrons scattered off ions. The evolution of footpoint sources from asymmetric to symmetric brightness can be seen as an evidence for different injection conditions of high energy electrons along the two legs of the loop system (Siarkowski & Falewicz 2004) which could be mainly because of the highly complicated systems of loops. Between the interval characterized by peaks B and C, we find a fast upward movement of X-ray looptop source. This upward growth indicates progression of magnetic reconnection in the higher coronal loops rooted successively further apart from the magnetic inversion line. On the other hand the lower loops eventually cool down (and fade away) and begin to be visible in low energies in UV and Hα lines. The structure of flaring region seen in Hα filtergrams at this stage also reveal a loop system connecting two Hα flare ribbons and is very similar to the 1600 Å images. We find that intense emission is produced from the top of the Hα loops. The appearance of bright looptop source in Hα emission against the solar disk is rather an unusual feature and considered as an evidence for high pressure, i.e. high density ($n \gtrsim 10^{12}\ cm^{-3}$) in the observed postflare loops (Heinzel and Karlický 1987).

3.3. Overall picture of flare evolution

This paper presents a unique set of observations of a flare event which shows two distinct phases in terms of X-ray energy release process. In Figure 13 we present two cartoons to depict the flare evolution during first and second phases. The first phase shows thermal emission from a LT source that exhibits unusually long duration of altitude decrease for 11 minutes. The EUV images of the flare region from TRACE show high temperature (15-20 MK) plasma emission from the X-ray LT source location. This TRACE 195 Å LT source also shows altitude decrease consistent with X-ray LT source motion. We present the most clear observations of loop shrinkage in direct EUV images. Further the observations of the first phase contains evidence for collapsing magnetic trap effect. However, the multi-wavelength observations described in this first or initial stage suggest the need of more realistic model for the evolution of magnetic field configuration to account for downward motion of LT source. We believe that a super-hot turbulent-current layer model could provide a plausible explanation for the production of hot and super-hot plasmas and the loop-top evolution (shrinkage) during the initial phase of eruptive flares (Somov 2006).

On the other hand, the second phase of flare evolution is dominantly non-thermal in nature with high energy hard X-ray emission from two foot-point sources. The multi-wavelength observations of the event during this phase are nearly consistent with the "stan-

dard model" of solar flares. At least this seems to be fairly true in the later stages when the primary energy source (i.e., reconnection site) is located high enough in the corona. In other words, the standard model of solar flares seems to be "asymptotically" true for large flares.

Part of this work was carried out when BJ was a Research Fellow at Aryabhatta Research Institute of Observational Sciences (ARIES), Nainital, India. We acknowledge the technical staff of ARIES Solar Tower Telescope for their assistance in maintaining and making regular solar observations. We acknowledge RHESSI and TRACE for their open data policy. RHESSI and TRACE are NASA's small explorer missions. This work has been supported by the "Space Weather Center Project" of KASI and KASI basic research fund. B. Somov thanks the Russian Foundation for Fundamental Researches.

REFERENCES

Brown, J. C. 1971, Sol. Phys., 18, 489

Brueckner, G. E. et al. 1995, Sol. Phys., 162, 357

Gallagher, P. T., Dennis, B. R., Krucker, S., Schwartz, R. A., & Tolbert, A. K. 2002, Sol. Phys.., 210, 341

Handy et al. 1999, Sol. Phys., 187, 229

Heinzel, P. & Karlický, M. 1987, Sol. Phys., 110, 343

Hudson, H. S. 1972, Sol. Phys., 24, 414

Hudson, H., Fletcher, L., Khan, J. I., & Kosugi, T. 2004, in Solar and Space Weather Radiophysics, eds. Gary, D. E. & Keller, C., Astrophysics and Space Science Library, 314, pp. 153

Hurford, G. J., Schmahl, E. J., Schwartz, R. A., et al. 2002, Sol. Phys., 210, 61

Ji, H., Huang, G., Wang, H. et al. 2006, ApJ, 636, L173

Joshi, B., Manoharan, P. K., Veronig, A., et al. 2007, Sol. Phys., 242, 143

Krucker, S., Hurford, G. J., & Lin, R. P. 2003, ApJ, 595, L103

Li, Y. P., & Gan, W. Q. 2005, ApJ, 629, L137

Li, Y. P., & Gan, W. Q. 2006, ApJ, 644, L97

Lin, R. P., Dennis, B. R., Hurford, G. J., et al. 2002, Sol. Phys.., 210, 3

Lin, J., Soon, W., & Baliunas, S. L. 2003, New A Rev., 47, 53

Liu, W., Jiang, Y. W., Liu, S., & Petrosian, V. 2004, ApJ, 611, L53

Liu, W., Petrosian, V., Dennis, B. R., & Jiang, Y. W. 2008, ApJ, 676, 704

Masuda, S., Kosugi, T., Hara, H., et al. 1994, Nature, 371, 495

Pant, P. 2006, JApA, 27, 293

Priest, E. R., & Forbes, T. G. 2002, A&A Rev., 10, 313

Sakao, T. 1994, PhD thesis, University of Tokyo

Siarkowski, M. & Falewicz, R. 2004, A&A, 428, 219

Smith, D. M., et al. 2002, Sol. Phys., 210, 33

Somov, B.V., & Bogachev S.A. 2003, Astronomy Letters, 29, 621.

Somov, B. V., Kosugi, T., Bogachev, S. A., Sakao, T., & Masuda, S. 2005, Adv. Space Res., 35, 1700

Somov, B. V., & Kosugi, T. 1997, ApJ, 485, 859

Somov, B. V. 2006, Plasma Astrophysics II: Reconnection and Flares (Springer)

Sui, L. & Holman, G. D 2003, ApJ, 596, L251

Sui, L., Holman, G. D., & Dennis, B. R. 2004, ApJ, 612, 546

Sui, L., Holman, G. D., White, S. M., & Zhang, J. 2005, ApJ, 633, 1175

Syrovatskii, S. I., & Shmeleva, O. P. 1972, Soviet Astronomy, 16, 273

Veronig, A. M., Karlický, M., Vršnak, B., Temmer, M., Magdalenić, J., Dennis, B. R., Otruba, W., & Pötzi, W. 2006, A&A, 446, 675

Warren, H. P., & Reeves, K. K. 2001, ApJ, 554, L103

This preprint was prepared with the AAS LaTeX macros v5.2.

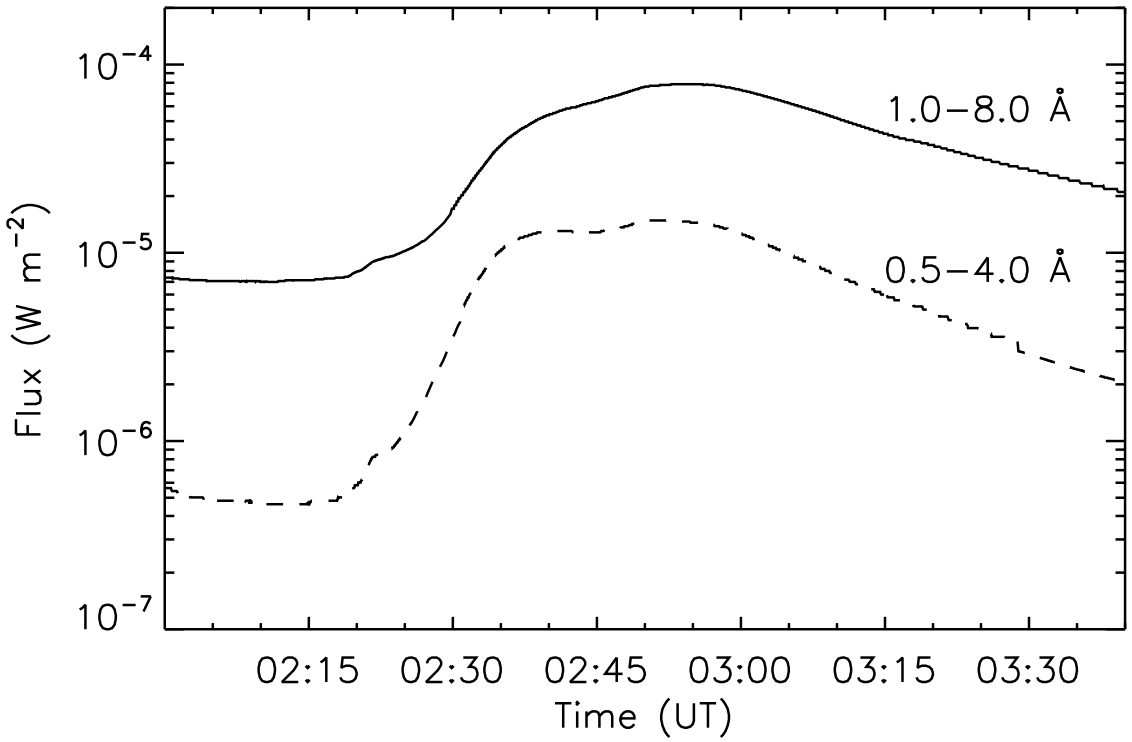

Fig. 1.— Soft X-ray light curves from GOES spacecraft for the period 02:00–03:40 UT. Solid and dashed lines indicate flux in 1–8 and 0.5-4 Å wavelength bands respectively.

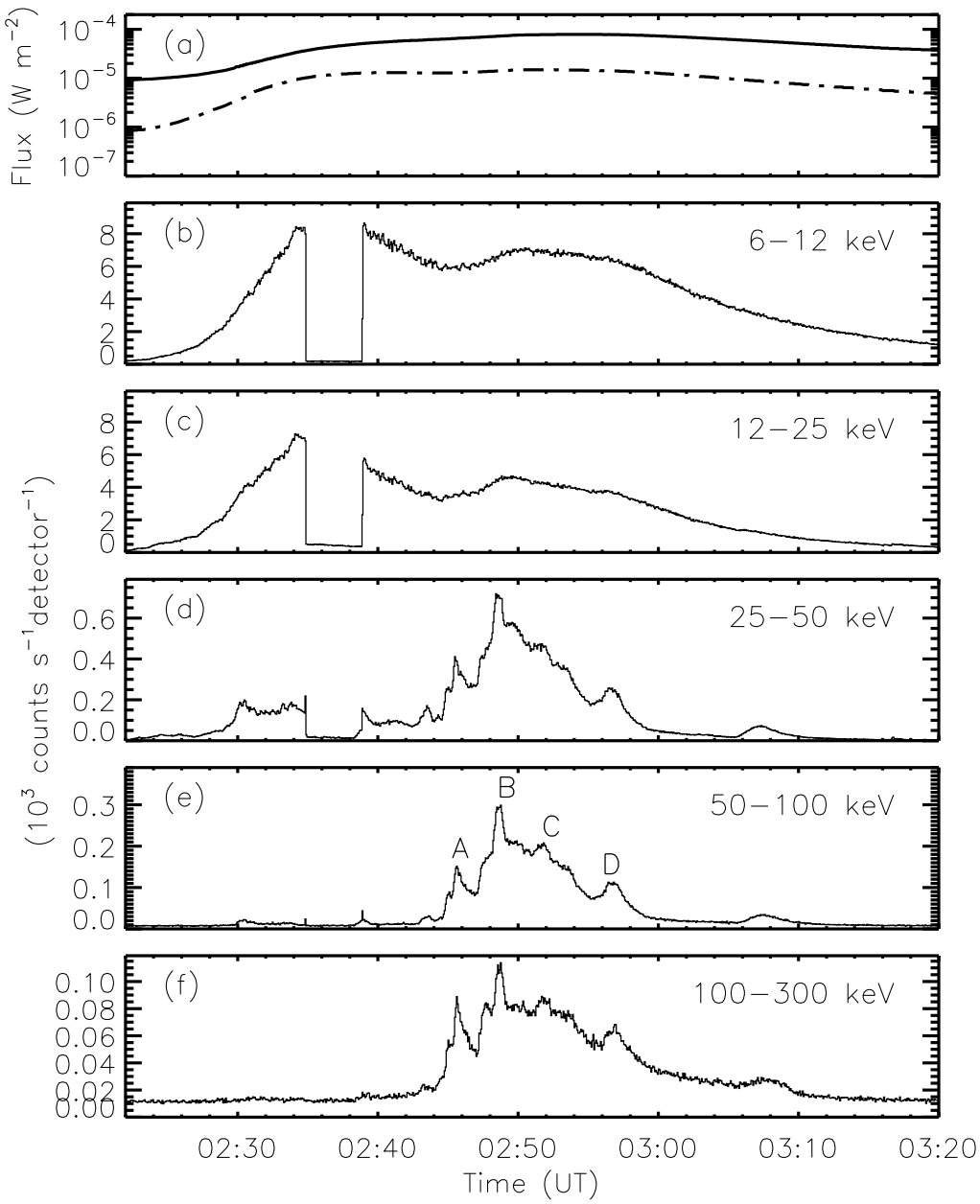

Fig. 2.— (a) GOES soft X-ray flux in 1–8 (solid) and 0.5-4 Å (dashed-dotted) channels. (b)–(e) RHESSI X-ray light curves in five energy bands with 4-s integration time. Panel (e) shows four peaks A, B, C, and D which are occuring simultaneously in all the high energy light curves ($\gtrsim$ 25 keV).

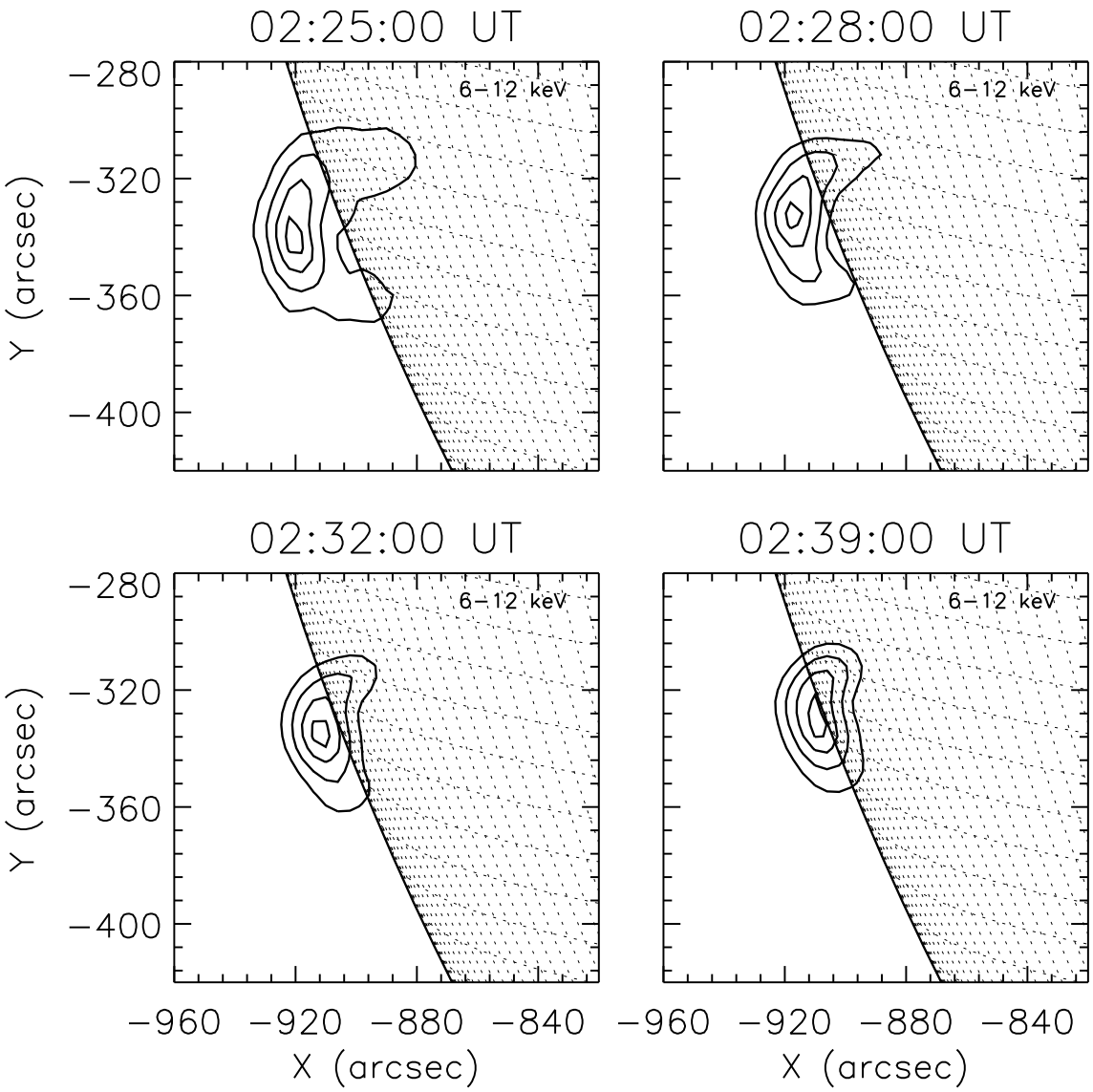

Fig. 3.— Sequence of RHESSI 6–12 keV images reconstructed with the CLEAN algorithm using grids 3 to 8 (excluding 7) and natural weighing scheme during the first phase of the flare showing the altitude decrease of the flaring loop system. The integration time for each image was 1 min. The contour levels are 40%, 60%, 80%, and 95% of the peak flux in each image. The solar limb and heliographic grids are also drawn in the images.

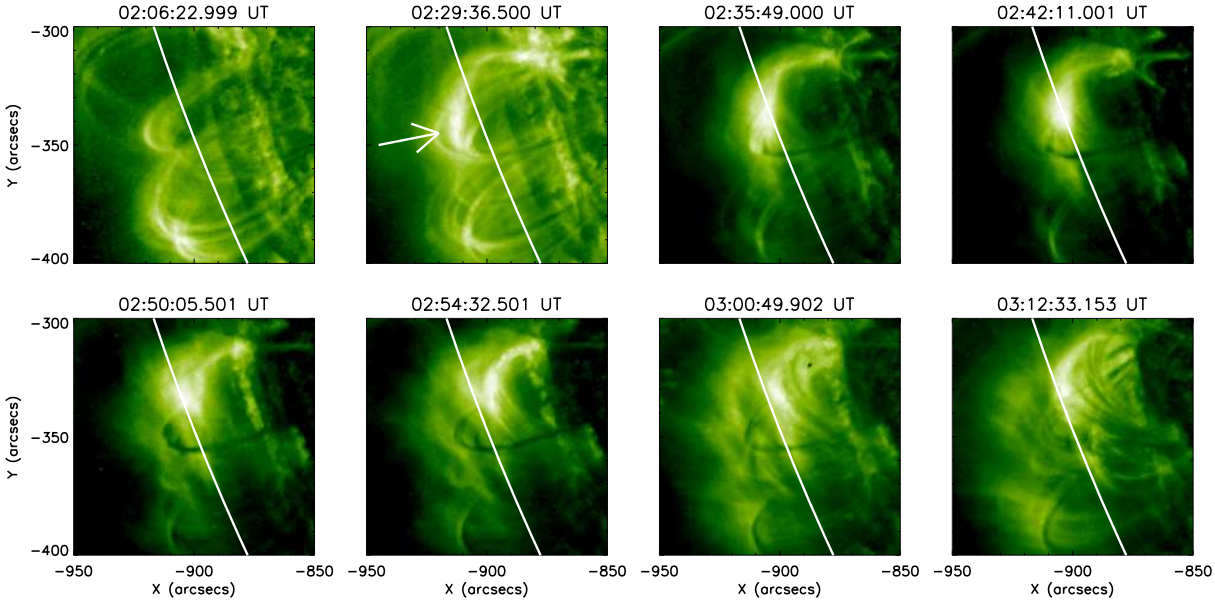

Fig. 4.— Time sequence of TRACE 195 Å images showing a closer view of coronal loops associated with the flaring region. The bright region at the top of the loop system is indicated by an arrow in the image at 02:29:36 UT. Note the pre-existing loop system and altitude decrease of the hot flaring loops (15-20 MK TRACE 195Å response) at the first flare phase, later ($\gtrsim$ 2:54 UT) followed by post-flare loops appearing dark and structured (1.5 MK TRACE 195 Å response).

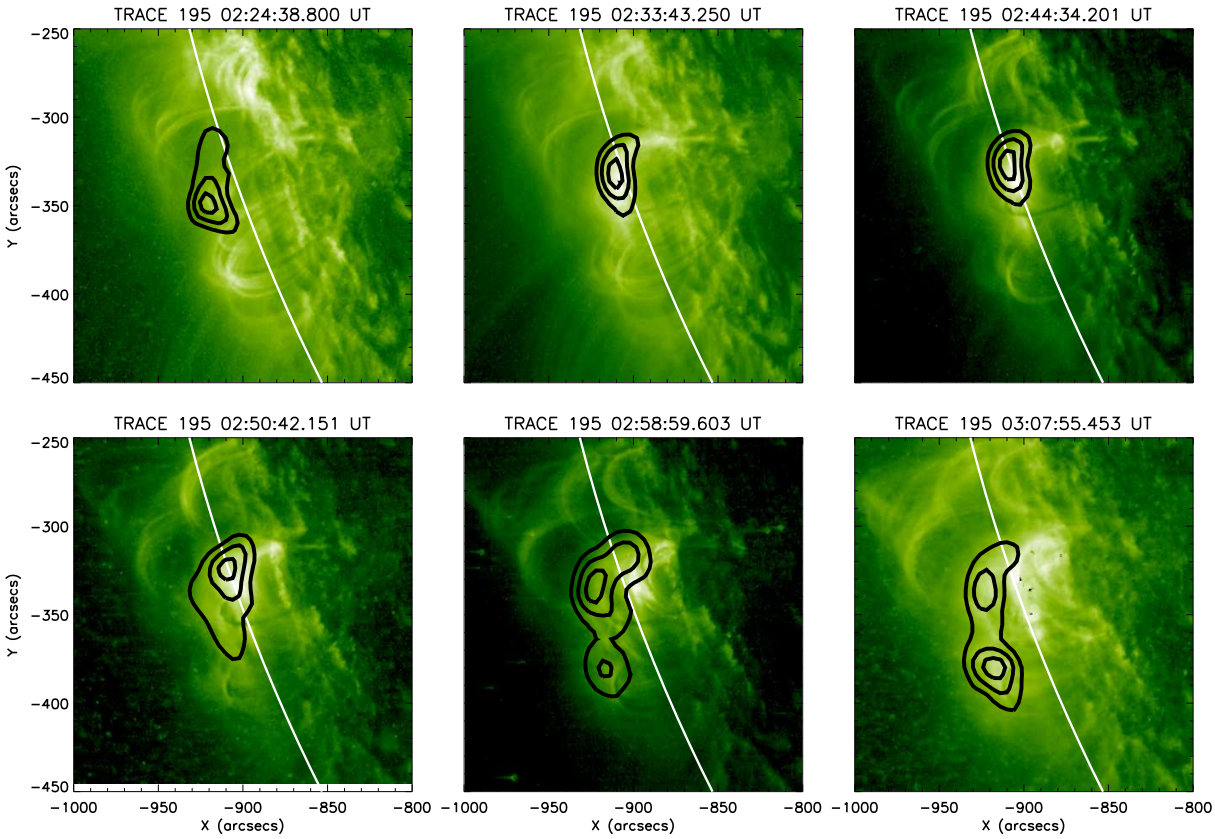

Fig. 5.— Sequence of TRACE 195 Å images overlayed by co-temporal RHESSI 6–12 keV images. RHESSI image parameters are the same as in Fig. 3. The contour levels are 50%, 70%, and 90% of the peak flux in each image.

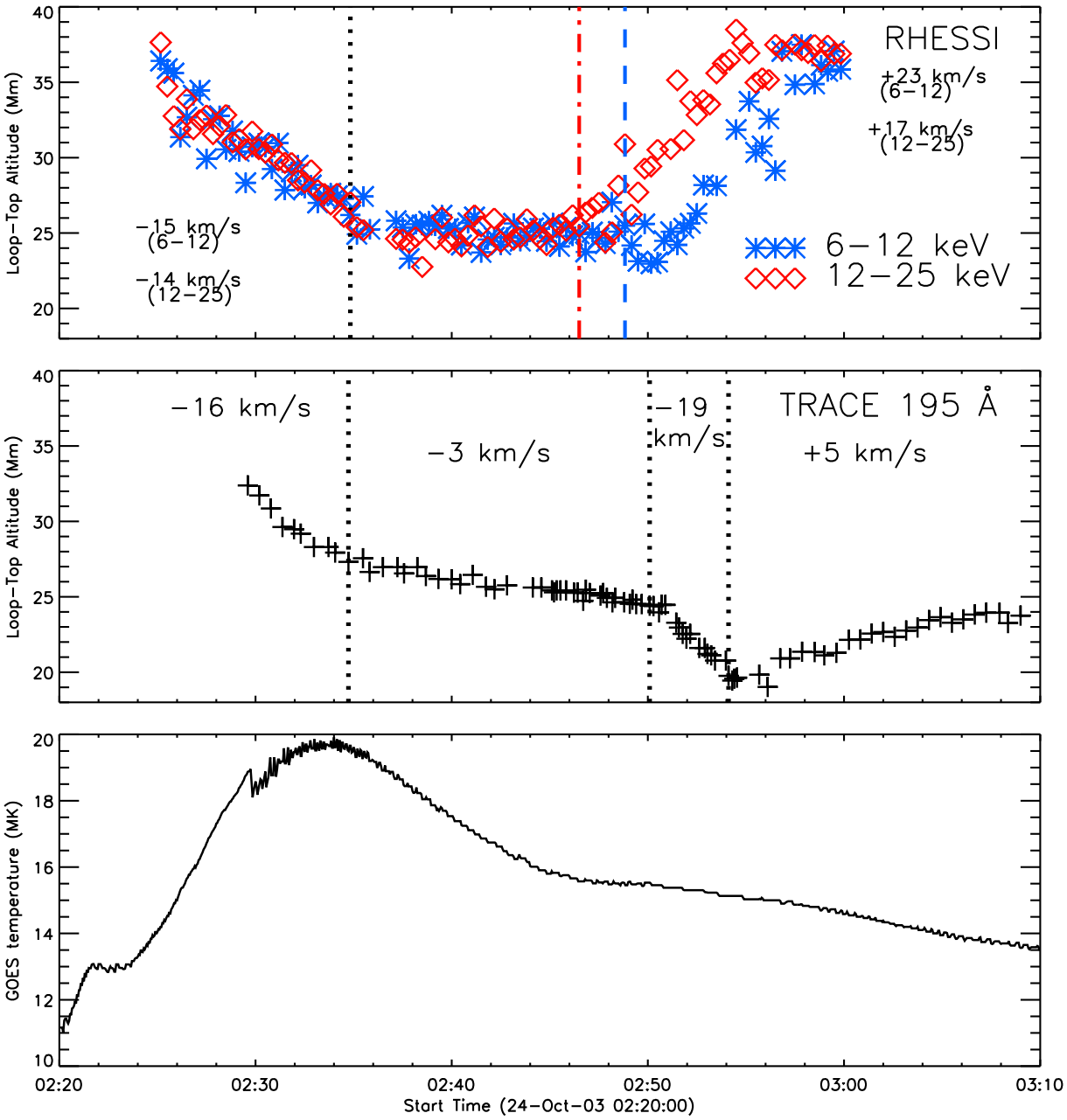

Fig. 6.— Top panel: Evolution of the altitude of the RHESSI LT source observed in the 6–12 and 12–25 keV energy bands. Note that the RHESSI LT source at 12–25 and 6–12 keV show upward motion after ∼02:46 and ∼02:49 UT respectively (start time is indicated by dash-dotted and dashed lines respectively). Middle panel: Evolution of the altitude of the TRACE 195 Å LT source. The mean velocities derived by linear fits to the altitude data in certain time interval (indicated by vertical lines) are annotated in the Figure. Bottom panel: Time profile of temperature derived from GOES-12 measurements.

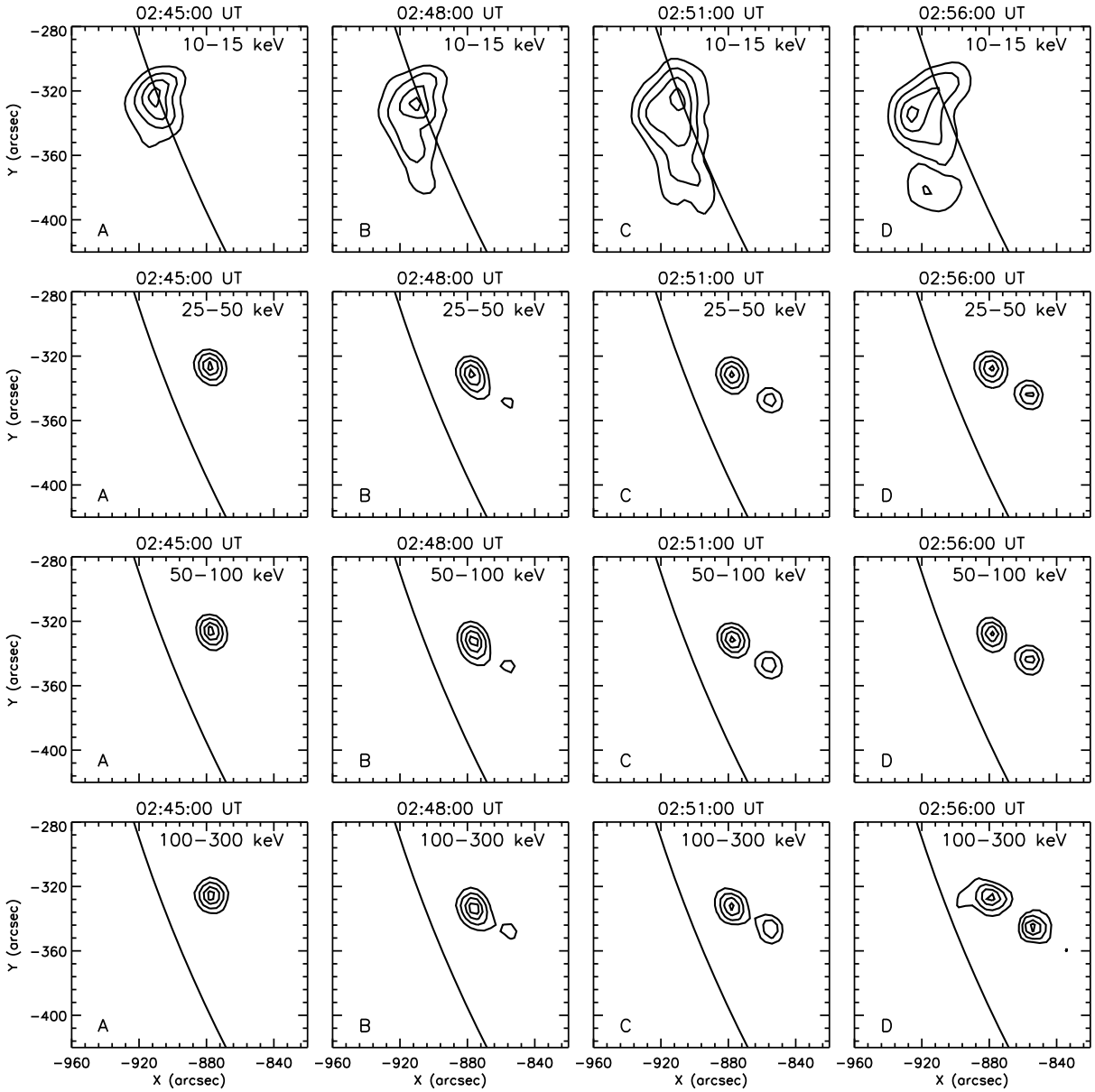

Fig. 7.— Sequence of RHESSI images in different energy bands from 10–300 keV. These peaks are indicated in Fig. 2. (panel e) with alphabets A, B, C, and D. The image restruction parameters are the same as in Fig. 3. The contour levels are 40%, 60%, 80%, and 95% of the peak flux in each image.

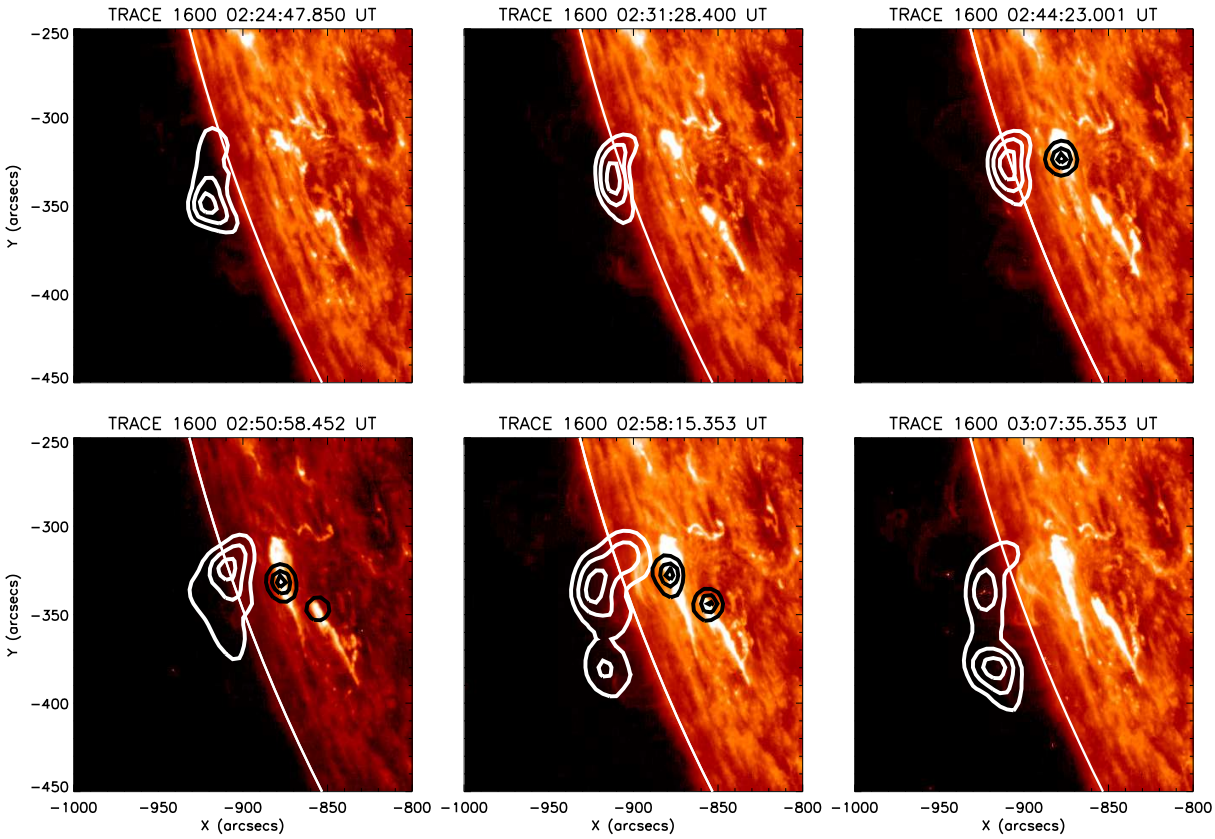

Fig. 8.— Sequence of TRACE 1600 Å images overlayed by RHESSI 6–12 keV (white contours) and 50–100 keV (black contours) images. RHESSI image parameters are the same as in Fig. 3. The contour levels are 50%, 70%, and 90% of the peak flux in each image.

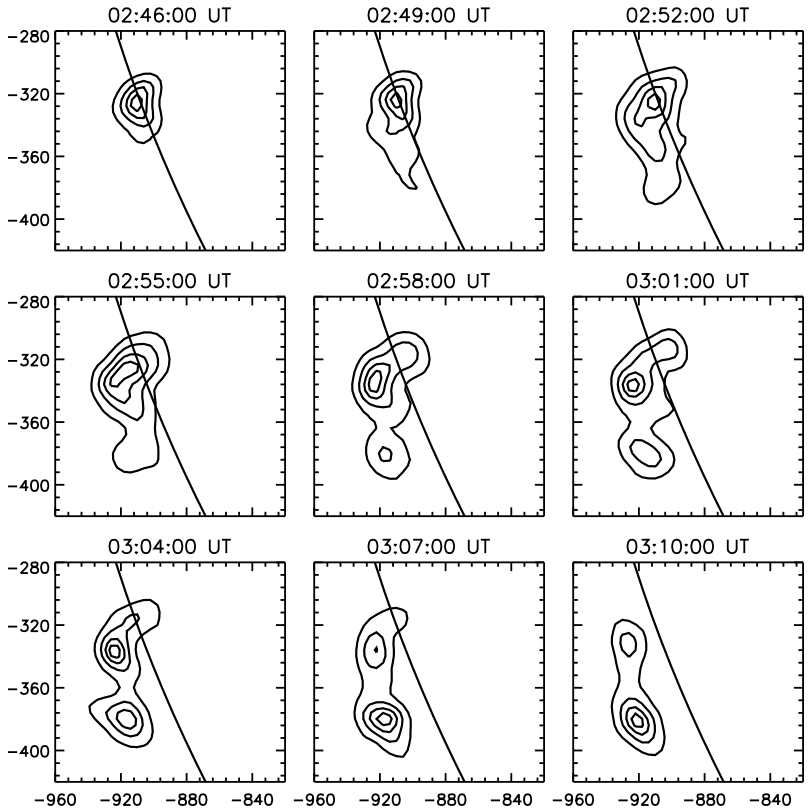

Fig. 9.— Sequence of RHESSI 6–12 keV images reconstructed during the second phase of the flare, showing the generally observed upward growth of the flare loop system. The imaging parameters are the same as in Fig. 3. The contour levels are 50%, 70%, 85%, and 95% of the peak flux in each image.

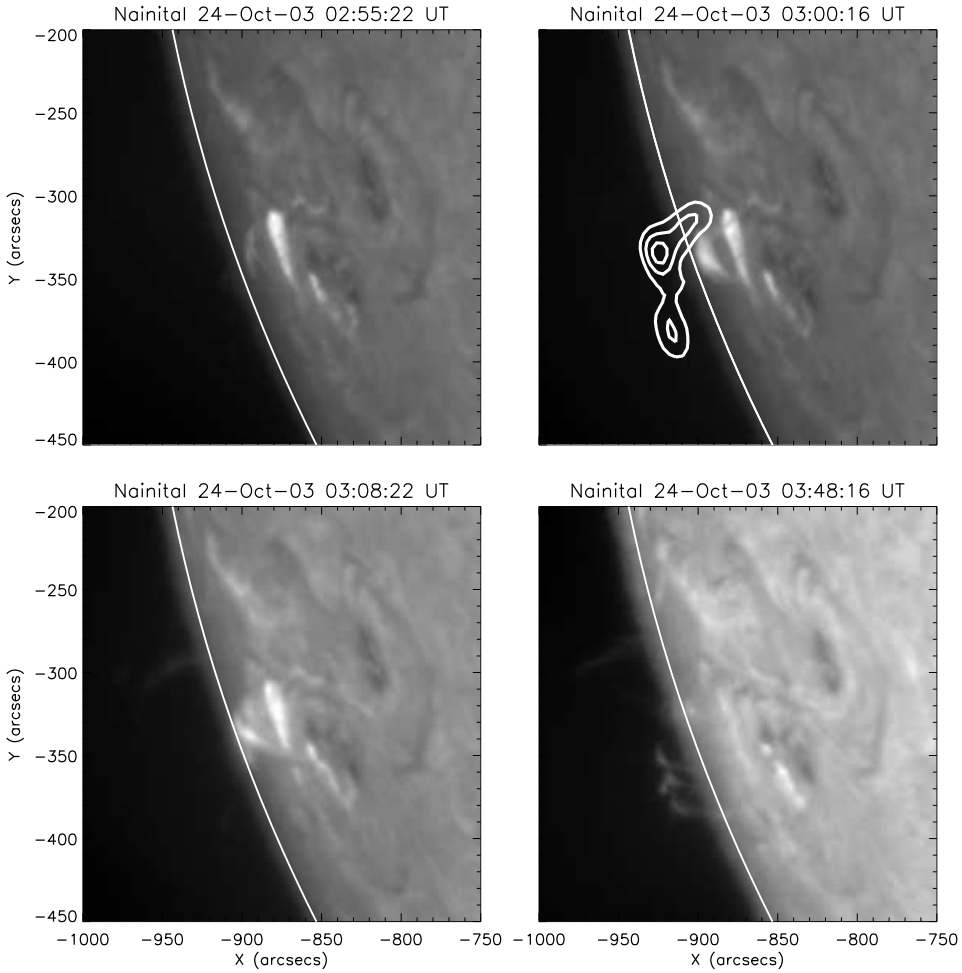

Fig. 10.— Some representative Hα images during the decline phase of the event. The white contours (only in top right panel) are RHESSI 6–12 keV image. The contour levels are 50%, 70%, and 90% of the peak flux. Note the Hα post-flare loops appearing bright against the disk, evidencing high plasma densities.

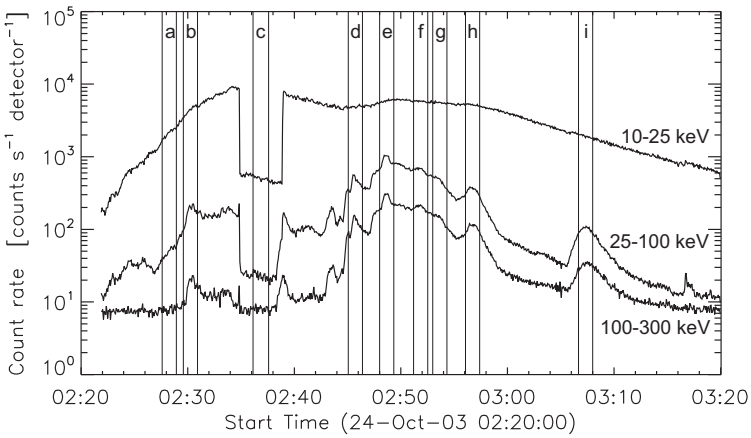

Fig. 11.— RHESSI light curves in three energy bands: 10–25, 25–100, and 100–300 keV. The time intervals during which the spectra shown in Fig. 12 were accumulated are indicated by vertical lines. Note that during 02:35–02:39 UT the RHESSI thick attenuator was in, whereas during all other times only the thin shutter was in.

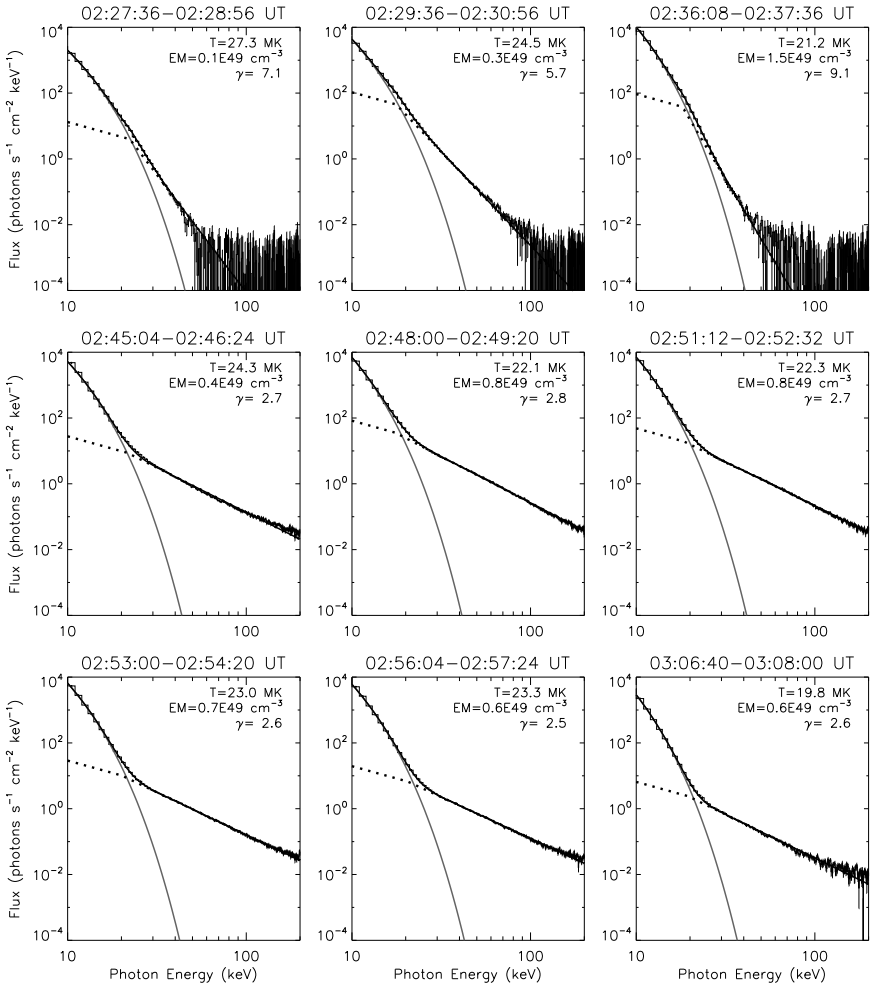

Fig. 12.— Spatially integrated background-subtracted RHESSI spectra derived during nine time intervals during the flare together with the applied spectral fits. The spectra in panels a)–c) were accumulated over 80 s during the first phase of the flare, panels d)–i) during the second phase of the flare. The spectra were fitted with a thermal bremsstrahlung model (grey lines) and a functional power-law with a turn-over at low energies (dotted lines). The black full lines indicate the sum of both components. The early spectra (a–c) were fitted in the energy range 10–50 keV, the spectra derived during the second phase of the flare (d–i) were fitted in the range 10–200 keV. Note that during time interval c, the RHESSI thick attenuator was in (A3 state), whereas during all other intervals only the thin attenuator was in (A1 state).

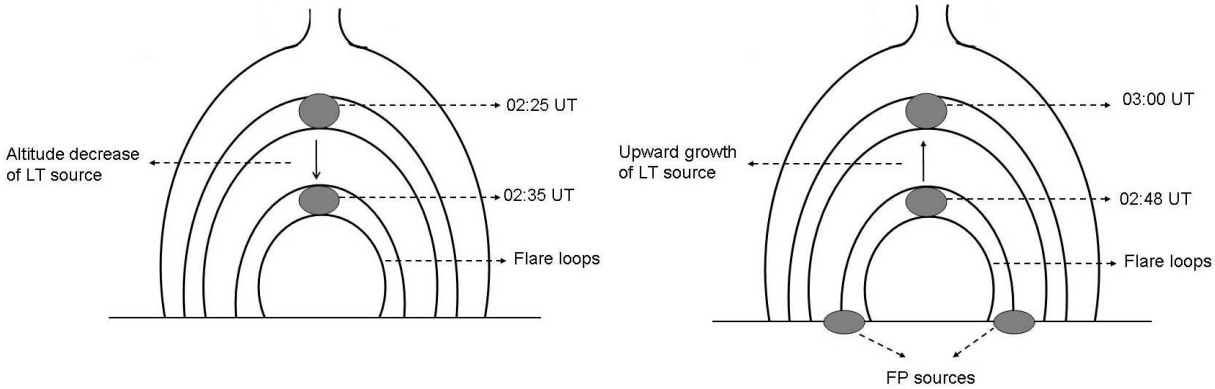

Fig. 13.— Schematic representation of the flare evolution during the first and second phases (left and right panels respectively) as revealed by RHESSI observations.